Proceedings of the Twenty-Third EGS Users' Meeting in Japan

August 8 - 9, 2016.
KEK, Tsukuba, Japan

Edited by

Y. Namito, H.Iwase, Y.Kirihara and H. Hirayama

High Energy Accelerator Research Organization

FOREWARD

The Twenty-third EGS Users' Meeting in Japan was held at High Energy Accelerator Research Organization (KEK) from August 8 to 9. The meeting has been hosted by the Radiation Science Center. More than 40 participants attended the meeting.

The meeting was divided into two parts. Short course on EGS was held at the first half of the workshop using EGS5 code. In the later half, 7 talks related EGS were presented. The talk covered the wide fields, like the medical application and the calculation of various detector responses *etc.* These talks were very useful to exchange the information between the researchers in the different fields.

Finally, we would like to express our great appreciation to all authors who have prepared manuscript quickly for the publication of this proceedings.

Yoshihito Namito
Hiroshi Iwase
Yo-ichi Kirihara
Hideo Hirayama
Radiation Science Center
KEK, High Energy Accelerator Research Organization

CONTENTS

INTRODUCTION OF CGVIEW 3.0.0

T. Sugita[1], Y. Kirihara[2], Y. Namito[2], and H. Hirayama[2]
[1]SSL, Tomobe 309-1716, Japan
[2]KEK, Tsukuba 305-0801, Japan

Abstract

The background of updating cgview code is described. Also, development and operating environment of cgview 3.0.0 is briefly mentioned.

1 Background

Cgview is a computer program to support egs5 Monte Carlo code.[1] Major capability of cgview is displaying calculation geometry, debugging of calculation geometry by using pseudo particle, and displaying calculated particle trajectories together with calculation geometry, which is called as "Display of *.pic file". Combinatorial geometry (CG) and Cylinder-slab geometry can be handled by cgview. Geometry of spheres of co-center and X-Y-Z mesh can be handled in display of *.pic file.

Cgview 2.* has been developed using Delphi and kylix, on windows and on linux respectively. Computational environment has changed largely; 64 bit CPU becomes common and windows 10 becomes popular. To catch up these change, cgview 3.0.0 was developed.

2 Version 3.0.0

Development environment of cgview 3.0.0 is as follows. As a development tool, Visual Studio 2012 was used. Cgview is written in C# language. OpenGL is utilized as a Computer graphics API (Application program interface).

Operating environment is Windows 7 and later version of windows. Then cgview 3.0.0 runs stand-alone because several necessary DLL files are included in cgview distribution. Latest version of cgview is 3.0.4, which includes any bug fix until now. As cgview handles CG and Cylinder-slab geometry, cgview can be used for support of other radiation transport simulation code which utilizes similar geometry package. Opening window of cgview is shown in Fig. 1. Cgview 3.0.0 for linux was not developed since the support of Kylix 3 was terminated.

To investigate the improvement of performance, we compared time to reading in *.pic file of 23.6 MB. As shown in Table 1, cgview 3.0.2 was faster than cgview 2.3.0 by factor 6 for reading in *.pic file. Thus, the improvement of performance of cgview 3.0.0 or later is clear.

Table 1: Comparison of time for reading in *.pic file
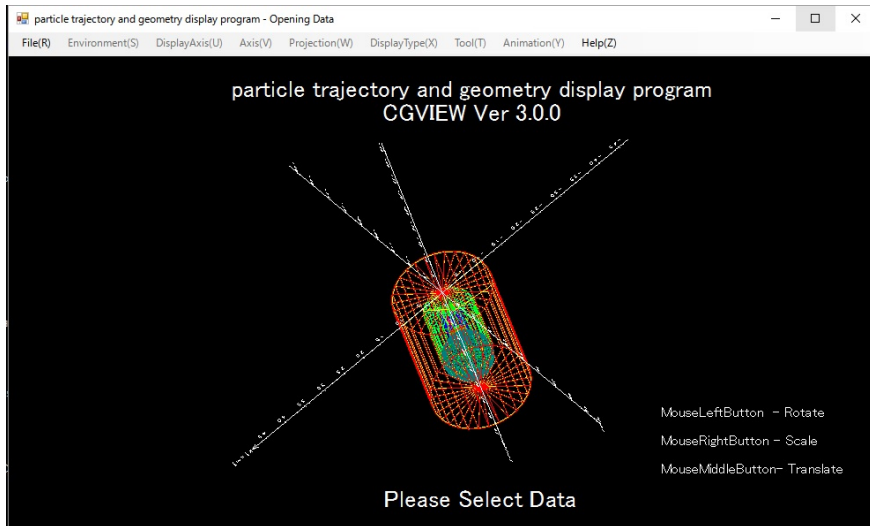
Version	Time (sec)
cgview 2.3.0	24
cgview 3.0.2	4

Figure 1: Opening window of cgview 3.0.0

References

[1] http://rcwww.kek.jp/research/egs/kek/cgview/ (2017.07.10 final confirmation)

ABOUT RELEASE OF BETA RAY LIBRARY OF EGS5

Y. Kirihara, H. Hirayama and Y. Namito

KEK, Tsukuba 305-0801, Japan

Abstract

Beta ray spectrum data for egs5 was prepared. For the spectral data, items included in ICRU Report 56 [2] and RADAR [3] were used. This is a short article for introduction because report is already written [1].

1 Source of beta ray spectrum data

1.1 ICRU56

In ICRU Report 56, β ray spectra from 36 nuclides are included. β ray energy is treated after divided by E_{Max}, which is a maximum β ray energy. Number of energy bin is 40. Number of β ray per decay per energy interval (=0.025) is given. If one divide the beta ray intensity data by 40, one gets the number of beta ray in an interval.

1.2 RADAR

RADAR is a β ray spectra data base developed by BNL National Nuclear Data Center. Data were taken from two references.

β ray spectra from 429 nuclides published in an article of Health Physics journal [4] is included. Energy interval of equal width is adopted. Number of energy interval is 20. Number of β ray whose energy corresponds to an interval is given for one decay.

β ray spectra from 34 nuclide published in BNL report [5] is also included. Energy bin width is in not equally spaced and number of energy intervals changes depending on nuclides. We did not include this part of data into egs5 beta ray library.

2 Comparison of β spectra from 32 nuclides in both ICRU-56 and RADAR

We compared beta ray spectra for 32 nuclides which both ICRU-56 and RADAR have. We also compared simplified formula calculation program (Beta CDF code) published in SLAC-TN-92-1 [6] as reference values. With respect to nuclides other than ^{210}Bi and ^{137}Cs, ICRU-56 data and RADAR data agree within several %.

About ^{210}Bi, RADAR data and SLAC-TN-92-1 are almost identical. Unlike the ICRU Report 56, the data of JAERI 1347 [8], which is the original data of the ICRP-107 data issued in 2007 [7], matches the RADAR data. ICRU-56 is a calculation adjusted to reproduce the measured spectrum, whereas RADAR is a purely theoretical calculation, which is explained in JAERI 1347. Which one to use is up to the judgment of the user.

About ^{137}Cs, the difference is not as large as ^{210}Bi, but the difference is bigger than other nuclides. Problems in the spectrum of ^{137}Cs of ICRU-56 are discussed in JAERI 1347 and use of RADAR is recommended.
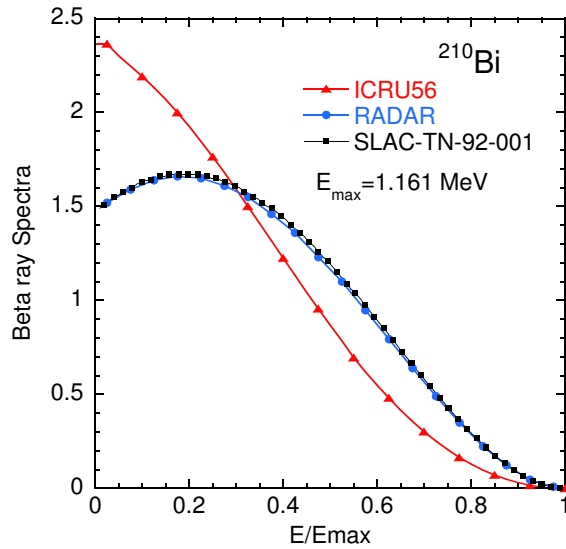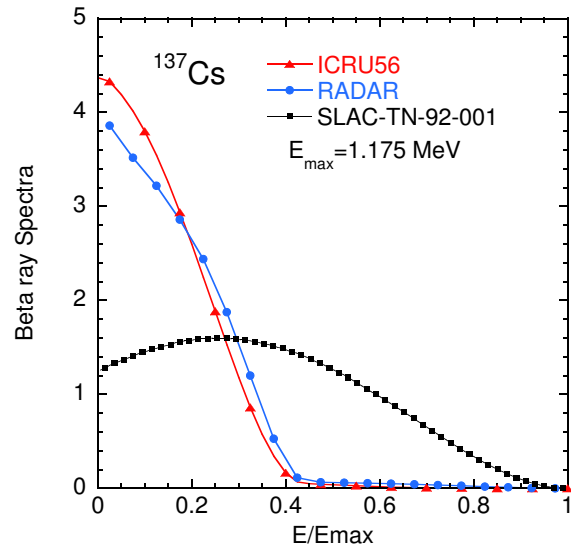
Figure 1: Comparison of beta spectrum from ^{210}Bi

Figure 2: Comparison of beta spectrum from ^{137}Cs

3   Sample code

Sample user code `ucicru56.f` and `ucradar.f` are written and distributed to use beta ray spectra data of ICRU-56 and RADAR, respectively.

Appendix

Following fortran programs were used to specify file name from key board.

For g77 compiler or any fortran compiler,

```
      character*10 atom
      character*72 filename
      write(6,'(A)')
   *    ' Key in atomic name and mass number like Sr-90'
      read(5,*) atom
      do i=1,10
        if(atom(i:i).eq.' ') go to 10
      end do
10    ii=i-1
      filename='RADAR/'//atom(1:ii)//'.data'
      open(2,file=filename,STATUS='old')}
```

For fortran compiler after Fortran 90,

```
      character*10 atom
      character*72 filename
      write(6,'(A)')
   *    ' Key in atomic name and mass number like Sr-90'
          read(5,*) atom
      filename='RADAR/'//trim(adjustl(atom))//'.dat'
      open(3,file=filename,STATUS='old')}
```

References

[1] Y. Kirihara, H. Hirayama and Y.Namito, "β-ray Spectrum Data for egs5 based on ICRU-56 or RADAR", KEK Report 2016-2, KEK (2016).

[2] "Dosimetry of External Beta Rays for Radiation Protection", ICRU Report 56.

[3] http://www.doseinfo-radar.com/RADARDecay.html (2017.06.29 final confirmation)

[4] K. F. Eckermanm R. J. Westfall, J. C. Ryman, and M. Cristy, "Availability of Nuclear Decay Data in Electronic Form, Including Beta Spectra not Previously Published", Health Phys. **67(4)**, 338-345 (1994).

[5] T. W. Burrows, "The Program RADLST", Brookhaven National Laboratory Report BNL-NCS-52142 (1988).

[6] W. R. Nelson and J. Liu, "Sampling the Fermi distribution for β-decay energy into EGS4", Stanford Linear Accelerator Center Report SLAC-TN92-1, June 1992, December 1997 (Rev).

[7] "Nuclear Decay Data for Dosimetric Calculations", ICRP Publication 107, Annals of ICRP, 38 (2008).

[8] A. Endo, Y. Yamaguchi and K. F. Eckerman, "Nuclear Decay Data for Dosimetry Calculation Revised Data of ICRP Publication 38", JAERI 1347, Japan Atomic Energy Research Institute (2004).

Investigating the characteristics of beams from a clinical linear accelerator for clinical dose calculations.

K. Masaki[1], S. Dobashi[1], Y. Ishizawa[1], K. Sato[2],
N. Kadoya[2], K. Ito[2], M. Chiba[2], and K. Takeda[1].

[1]Health Sciences, Tohoku University Graduate School of Medicine,
Sendai, 980-8574, Japan
[2]Tohoku University Hospital, Sendai, 980-8574, Japan
e-mail: k.masaki@med.tohoku.ac.jp

Abstract

For the accurate dose calculations in radiation therapy, the characteristics of beams from a clinical linear accelerator must be properly integrated in dose calculation algorithms. The purpose of this study was to investigate the characteristics of beams from a clinical linear accelerator and to use it for dose calculations in the clinical situation. To investigate the beam characteristics, Monte Carlo simulation was performed for the 6 MV photon beams from the CL23EX (Varian Medical Systems, Palo Alto, USA) accelerator by using EGS5. The validity of the simulation was confirmed by calculating the dose distributions in water based on the simulated phase space data and comparing them with the measured values in terms of the percentage depth dose (PDD) and the off axis ratio (OAR). In the evaluation of the PDD, calculated PDDs and the measured values were consistent within 1% after the buildup region. In the evaluation of the OAR, calculated OARs and the measured values were consistent within 3% in the radiation field. The results of the accelerator simulation were in good agreement with measurements. In addition, dose distributions of the clinical treatment plan were calculated based on the phase space data and compared with the one calculated by Varian Acuros XB algorithm. The local error of the dose at the isocenter was 0.11%. The gamma passing rate of the 3D gamma analysis in the patient body contour was 97.19% with 3%3mm criteria. These results showed that the dose distribution in the clinical situation could be calculated using MC without being inferior to commercial treatment planning system.

1. Introduction

Monte Carlo (MC) method is the most accurate dose calculation method and recognized as a gold standard in radiation therapy. MC method can calculate accurate radiation delivery; however, if characteristics of inputted beams (e.g., energy spectra, angular distributions, etc.) are incorrect, calculated dose calculations will include errors. Several studies have reported how to investigate the characteristics of beams by using MC method [1-4]. The purpose of this study is to investigate the characteristics of beams from a clinical linear accelerator by using MC method and to calculate the dose distribution in the clinical situation bases on the derived beam characteristics.

2. Materials and Methods

2.1 MC simulations for the clinical linear accelerator.

The MC code EGS5 was used to simulate 6 MV photon beams from the CL23EX accelerator (Varian Medical Systems, Palo Alto, USA). The geometrical details of the accelerator head were obtained from manufacturers' specifications [5]. The schematic overview of the simulated geometry is shown in Fig. 1.

The accelerated electrons impinging on the target were affected by the bending magnet. This effect was represented by parameters of the electrons incident on the target [6]. Kinetic energy was represented as a Gaussian distribution with a mean $\mu =$ 6.18 MeV and a standard deviation $\sigma = 0.053$ MeV. The focal spot was represented as a 2D Gaussian distribution with a mean $\mu_x = 0$ mm and a standard deviation $\sigma_x = 0.6866$ mm in the x-direction, a mean $\mu_y = 0$ mm and a standard deviation $\sigma_y = 0.7615$ mm in the y-direction.

Simulations were divided into 2 sections. The first section (simulation1) was from the target to under the flattening filter, the second section (simulation2) was from under the flattening filter to the isocenter plane. The first section was "field-independent" part and the second section was "field-dependent" part. The geometrical setup for the simulation1 remains unchanged for any field condition. To reduce the calculation time, particles crossing the scoring plane1 were scored in the PSF only once, and the obtained PSF was repeatedly used for the second section. In the second section, 3 types of square fields (Jaw 3×3 cm², 5×5 cm², 10×10 cm²) were simulated, and particles crossing the scoring plane2 were scored in the another PSF.

The particle information scored in the PSF was as follows: particle charge (iq), energy (e), particle position (x,y) and direction vector (u,v), interaction history (latch), z-coordinate of last interaction (zlast), weight (wt). The file format was binary. Record

length of iq was 1 byte and the others were 4 bytes. Therefore, record length was 33 bytes per particle.

The cut off energies were AE = 0.700 MeV and AP = 0.010 MeV. In the first section, variance reduction technique "bremsstrahlung splitting" was used with splitting factor 50. The PSF at the scoring plane1 contained 1.44×10^9 particles, and these were used for the simulation2 12 times with different random seeds in each field.

2.2 Dose calculations in water phantom.

To confirm the validity of the simulations, dose distributions in water were calculated by using derived PSF at the scoring plane2. The phantom size was $27.5 \times 27.5 \times 27.5$ cm^3 and the calculation grid was $0.5 \times 0.5 \times 0.5$ cm^3. The PSF obtained for the fixed jaw openings in the section2 was used 12 times with different random seeds in each field again. The cut off energies were AE = 0.521 MeV and AP = 0.010 MeV.

2.3 Measurements.

The percentage depth dose (PDD) and the off axis ratio (OAR) were measured in water. The water phantom was Blue Phantom^2 (IBA Dosimetry, Schwarzenbruck, Germany). As detectors, the IBA CC04 (IBA Dosimetry) ionization chamber was used for the measurements of the PDD, the EDGE Detector (Sun Nuclear Corporation, Melbourne, USA) diode detector was used for the measurements of the OAR, and the IBA CC13 (IBA Dosimetry) ionization chamber was used to correct for fluctuations of the output. Measured fields were Jaw 3×3 cm^2, 5×5 cm^2, 10×10 cm^2 square fields. OARs were measured in 4 depths (1.5 cm, 5.0 cm, 10 cm, 20 cm) in each field.

2.4 Dose calculations of the clinical treatment plan.

Dose distributions of the clinical treatment plan were calculated based on the PSF. The clinical situation was stereotactic body radiation therapy (SBRT) for the non-small cell lung cancer. The prescribed dose was 40 Gy in 4 fractions to cover 95% of the planning target volume (PTV). Treatment beams were non-coplanar 7 fields with 6 MV photon.

Calculation geometry was obtained from CT images used in the clinical treatment planning. The planning CT images were resampled to $0.25 \times 0.25 \times 0.25$ cm^3 isotropic voxels. Hounsfield Unit (HU) values assigned to each voxel were converted to the mass densities using a calibration curve shown in Fig. 2 following the procedure used in Varian Acuros XB algorithm [7]. Assigned materials were determined by the mass densities. The relationship between assigned materials and mass densities is shown in Table. 1. If a mass density was in an overlapped region, an assignment material would

be a mixture of two materials and its composition was calculated as a weighted average.

Irradiation parameters (e.g., field size, gantry angle, monitor unit (MU), etc.) were set up according to DICOM-RT plan files. Unlike water cases, PSF at the scoring plane1 was used directly for clinical dose calculations. According to field conditions, actual heights and openings of the collimators were calculated. Checkpoints were provided at the calculated heights: upper edge of the Jaw, lower edge of the Jaw, and center of the MLC thickness. At the checkpoints, it was checked whether particle positions were in collimator openings or not. Particles only in collimator openings were used for dose calculations and the others were ignored. By omitting collimator simulations, calculation time was reduced. Also, because the voxel size was smaller than water cases, additional accelerator simulations were performed until the number of particles at the scoring plane1 reached 3×10^9 in order to reduce the variance of the PSF.

The number of histories was 5×10^8 in each field, and the maximum variance of the absorbed dose in the PTV was less than 1.0% in each field. The cut off energies were AE = 0.521 MeV and AP = 0.010 MeV.

Calculated dose distributions were calibrated based on the MU values. The output of the CL23EX accelerator was 1 Gy = 129.5505 MU at 10 cm depth on the central axis in water when SSD = 90 cm and Jaw 10×10 cm². We performed a dose calculation of the same situation and derived the calibration factor which converts calculation results to the absorbed dose.

In clinical dose calculations, EGS5-MPI (Advanced Industrial Science and Technology: AIST) was used. 4 PCs with Intel Core i7-6700 (maximum frequency 4 GHz, quad-core) were used for clinical dose calculations, and calculation time was about 24 hours to calculate all the 7 fields.

Dose distributions calculated by MC were compared with the one calculated by Acuros XB (ver. 11.0.42). Acuros XB is the grid-based Boltzmann solver algorithm. Several studies have reported that the accuracies of MC and Acuros XB are almost the same [8-10].

3. Results

3.1 Verification of the accelerator simulations.

Comparison between calculated PDDs and measured values is shown in Fig. 3. Also, comparison between calculated OARs and measured OARs in the x-direction is shown in Fig. 4. In both cases, the results were normalized at the 10 cm depth on the central axis. According to the International Atomic Energy Agency (IAEA) technical report [11],

calculated PDDs and OARs were in good agreement with measurements. The results of OARs in the y-direction were about the same as in the x-direction.

3.2 Dose calculations of the clinical treatment plan.
Dose distributions of the SBRT case calculated by MC and Acuros XB are shown in Fig 5. Also, subtractions of the dose distributions (Acuros XB − MC) are shown in Fig. 6. The dose at the isocenter calculated by MC was 45.83 Gy and Acuros XB was 45.78 Gy. In addition, the 3D gamma analysis was performed with threshold 10% of the maximum dose. Gamma passing rates in the patient body contour were 77.38% with 2%2mm criteria and 97.19% with 3%3mm criteria. In the PTV contour, it was 88.25% with 2%2mm criteria and 99.63% with 3%3mm criteria. These results showed good agreement between MC and Acuros XB.

4. Discussion

In accelerator simulations, parameters of the initial electron were determined by the information of the TrueBeam (Varian Medical Systems) accelerator, not CL23EX. Linear accelerators have individual differences. Because parameters of the CL23EX were unclear, we intended to adjust parameters of the TrueBeam so that the derived PSF conforms to measurements. However, it was in good agreement with measurements with initial parameters.

In clinical dose calculations, collimators were simplified representation. However, an actual MLC has a very complex structure. It causes typically phenomena that are called the rounded leaf end transmission, the tongue-and-groove effect, etc. Our model does not take into account its complex structure. Improving collimator models is one of the future works.

The particle information latch and zlast were not used for dose calculations. However, these information were important to analyze the characteristics of beams. Derived PSF will be used as the reference when determining beam parameters of other dose calculation algorithms.

5. Conclusions

We performed MC simulations for the clinical linear accelerator by using EGS5 and the characteristics of beams were determined. Derived characteristics were in good agreement with measurements. Finally, we calculated dose distributions of the clinical

treatment plan. Calculated dose distribution in the clinical situation was in good agreement with the one calculated by Acuros XB.

References

1) Radhe Mohan, Chen Chui, and Leon Lidofsky, "Energy and angular distributions of photons from medical linear accelerators", Medical Physics 12, 592–597 (1985).

2) George X Ding, "Energy spectra, angular spread, fluence profiles and dose distributions of 6 and 18 MV photon beams: results of Monte Carlo simulations for a Varian 2100EX accelerator", Phys. Med. Biol. 47, 1025–1046 (2002).

3) Jun Deng, Steve B Jiang, Ajay Kapur, Jinsheng Li, Todd Pawlicki and C-M Ma, "Photon beam characterization and modelling for Monte Carlo treatment planning", Phys. Med. Biol. 45, 411–427 (2000).

4) W. van der Zee and J. Welleweerd, "Calculating photon beam characteristics with Monte Carlo techniques", Medical Physics 26, 1883–1892 (1999).

5) Varian medical systems, "Monte Carlo Data Package High Energy Accelerator DWG NO 100040466-02 Rev2", CONFIDENTIEL.

6) Varian medical systems, "TrueBeam Monte Carlo Data Package" (2014).

7) Varian medical systems, "Eclipse Algorithms Reference Guide" (2013).

8) Oleg N Vassiliev, Todd A Wareing, John McGhee, Gregory Failla, Mohammad R Salehpour and Firas Mourtada, "Validation of a new grid-based Boltzmann equation solver for dose calculation in radiotherapy with photon beams", Phys. Med. Biol. 55, 581–598 (2010).

9) K. Bush, I. M. Gagne, S. Zavgorodni, W. Ansbacher, and W. Beckham, "Dosimetric validation of Acuros® XB with Monte Carlo methods for photon dose calculations", Medical Physics 38, 2208–2221 (2011).

10) S. A. M. Lloyd and W. Ansbacher, "Evaluation of an analytic linear Boltzmann transport equation solver for high-density inhomogeneities", Medical Physics 40, 011707-1–011707-5 (2013).

11) IAEA, "INDC International Nuclear Data Committee Phase-Space Database for External Beam Radiotherapy Summary Report of a Consultants' Meeting" (2005).
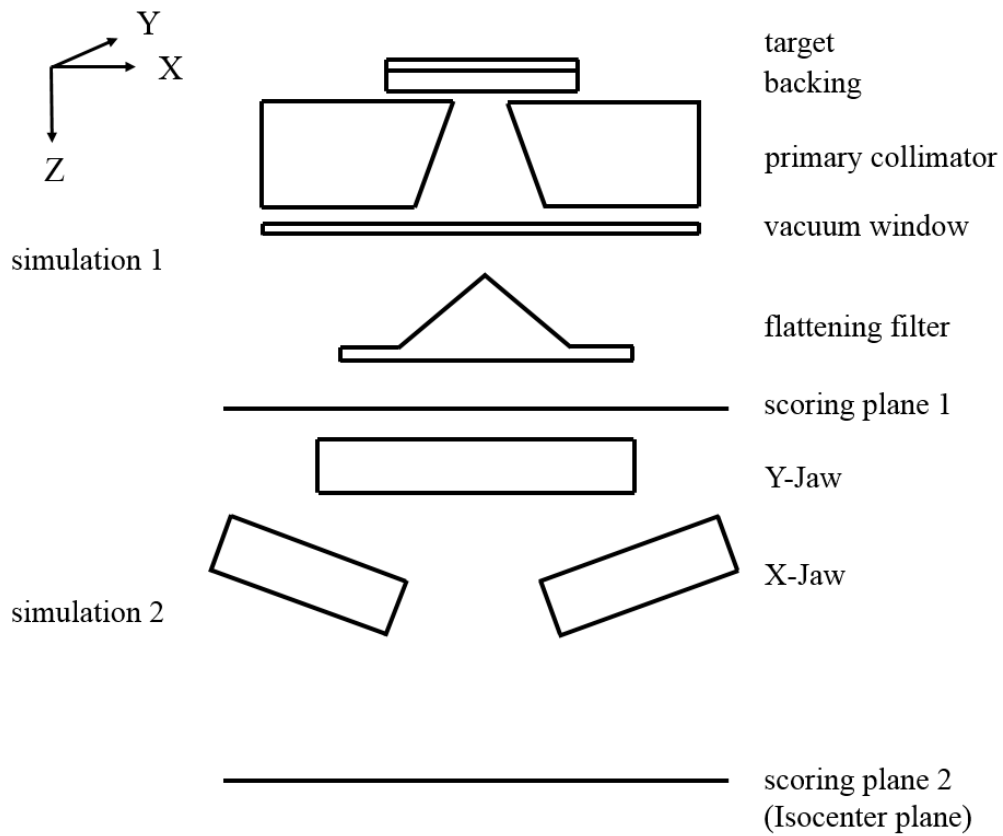
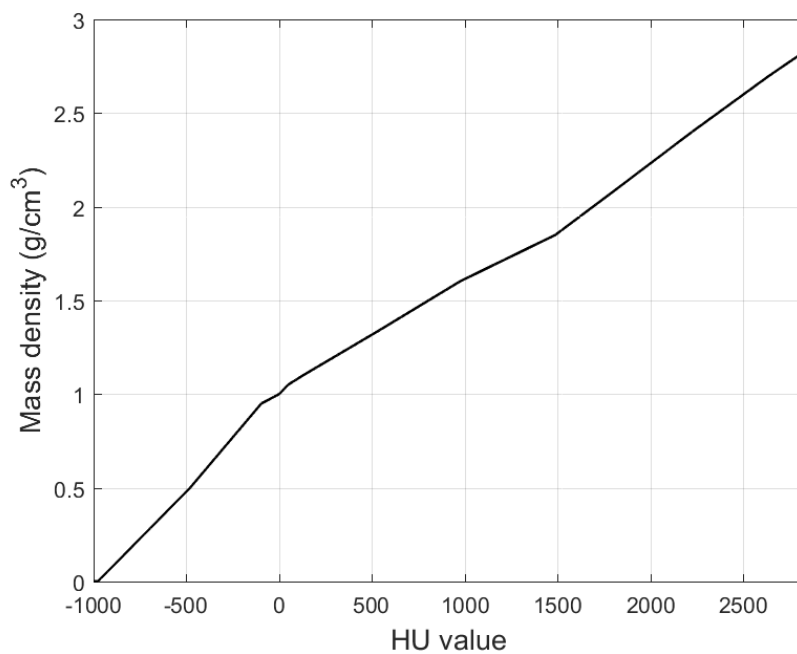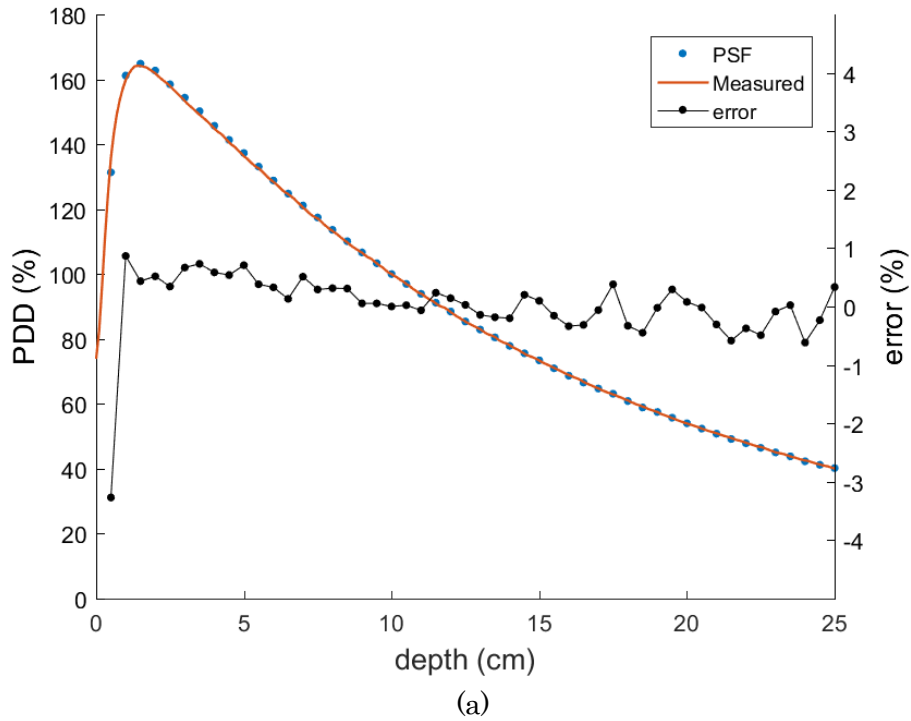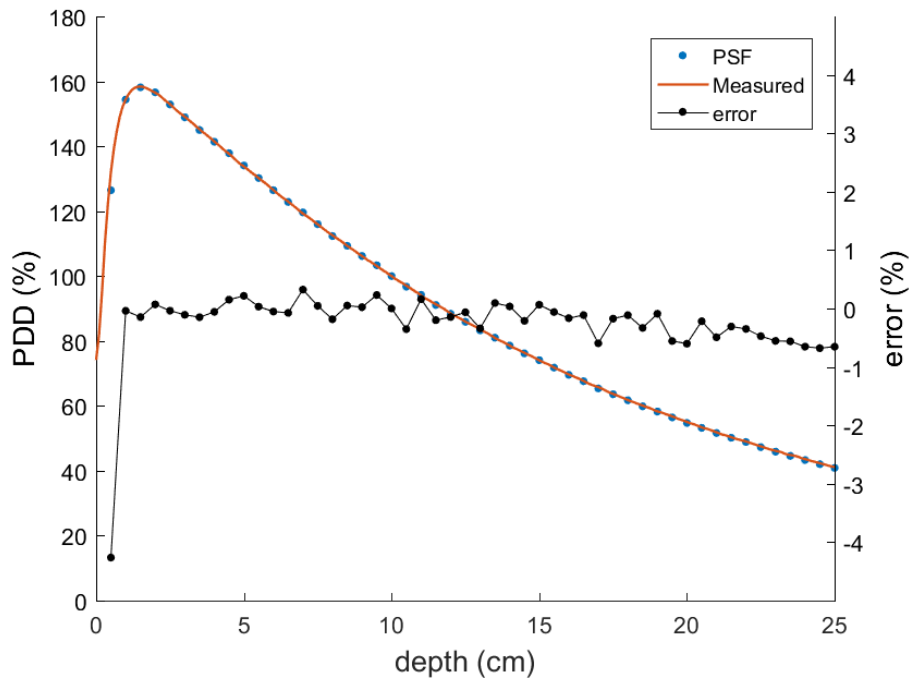Fig. 1 Schematic overview of the accelerator simulation.

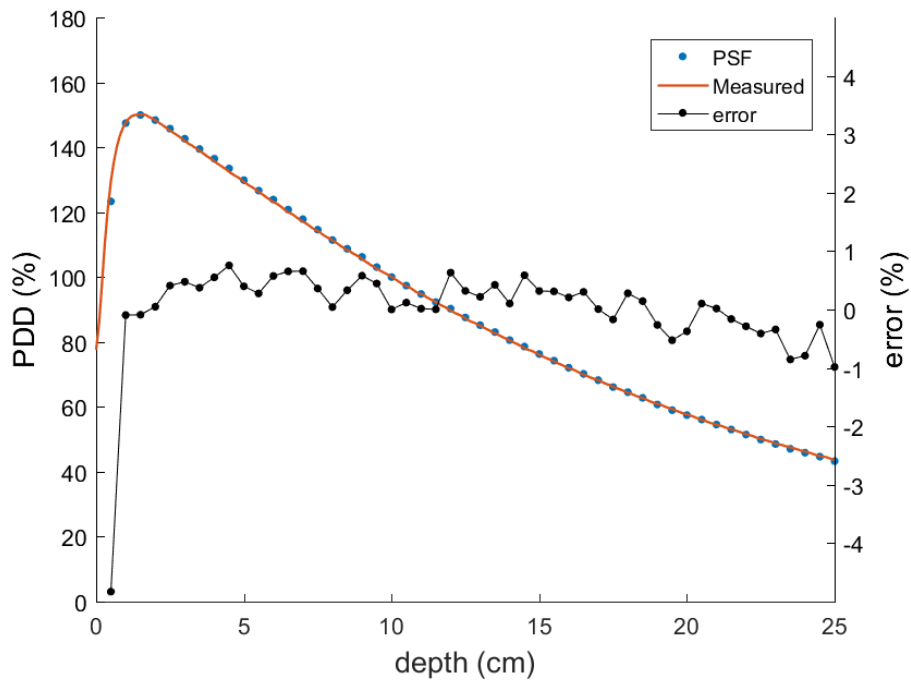Fig. 2 HU value-to-mass density calibration curve.

Table. 1 Relationship between assigned materials and the mass density.

	Mass density (g/cm^3)	
Material	minimum	maximum
Air (STP)	0.0012	0.0204
Lung (ICRP 1975)	0.0110	0.6242
Adipose Tissue (ICRP 1975)	0.5539	1.0010
Muscle, Skeletal (ICRP 1975)	0.9693	1.0931
Cartilage (ICRP 1975)	1.0556	1.60
Bone (ICRP 1975)	1.10	3.00

(a)

(b)
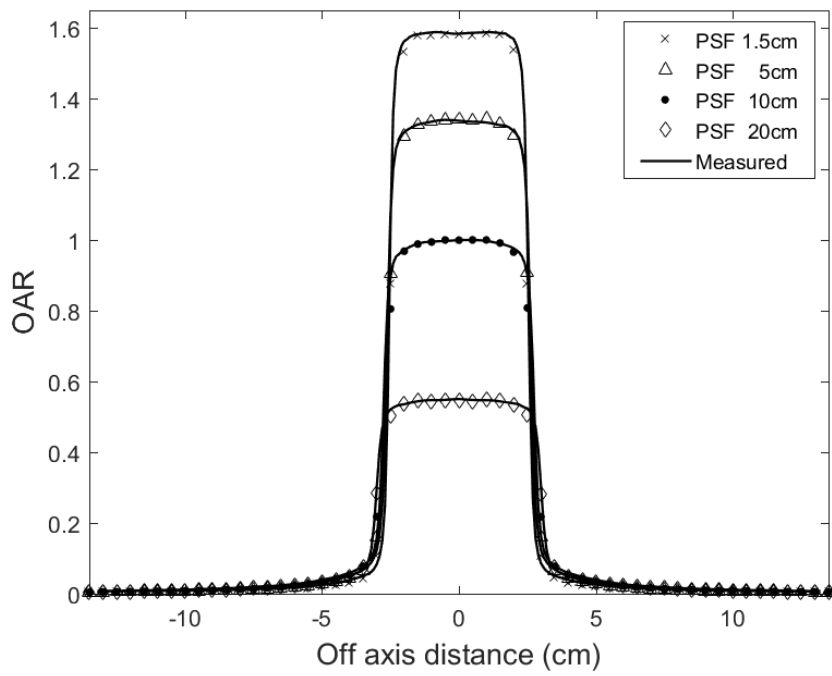

(c)

Fig. 3 Comparison between calculated PDDs and measured PDDs.

(a) 3×3 cm^2 (b) 5×5 cm^2 (c) 10×10 cm^2

(a)

(b)

(c)

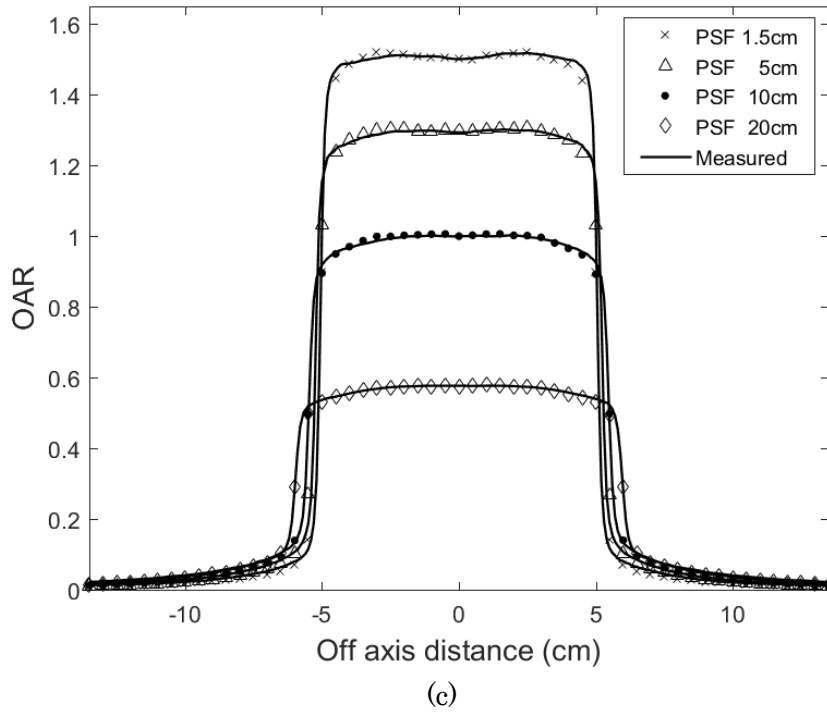Fig. 4 Comparison between calculated OARs and measured OARs.

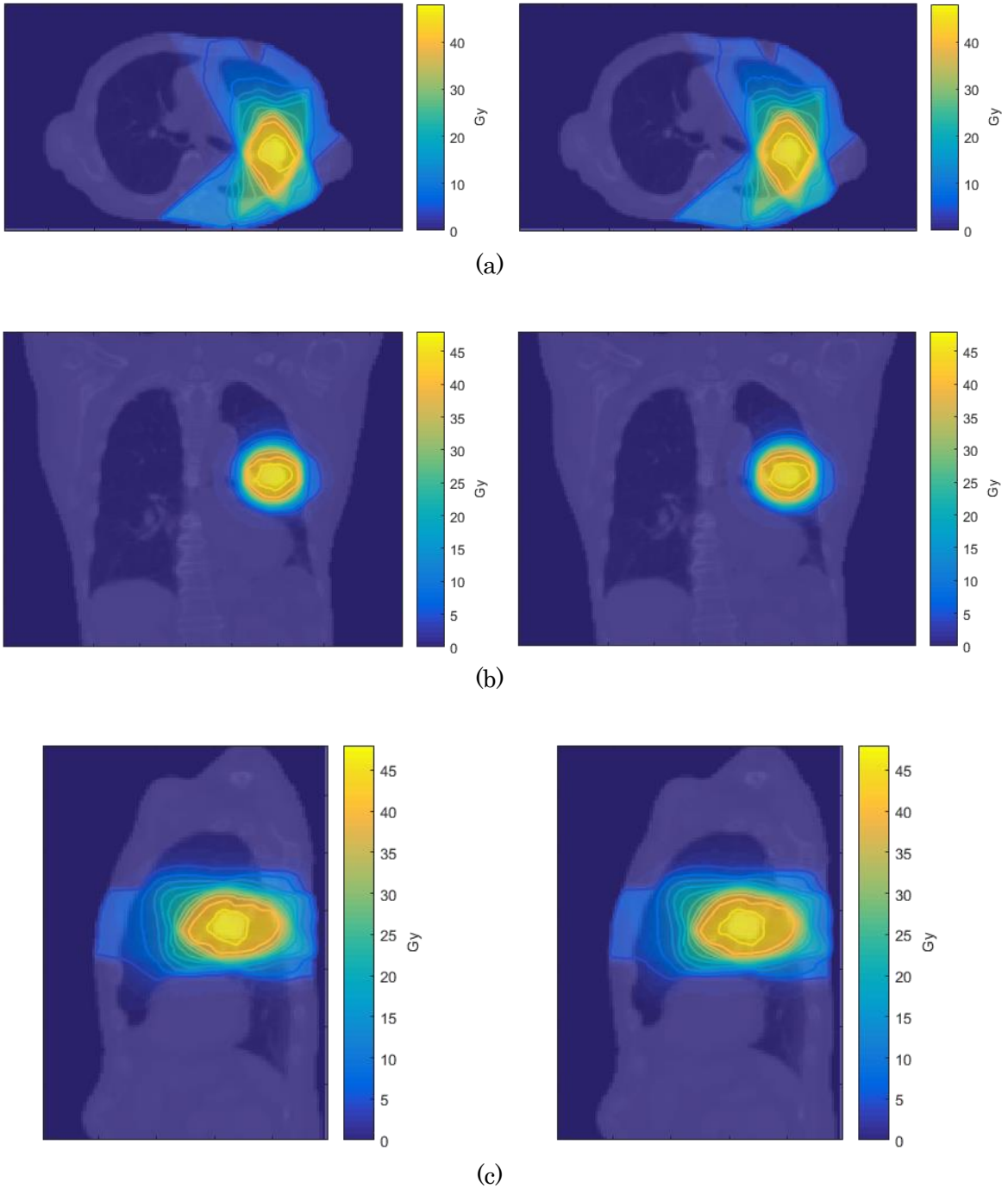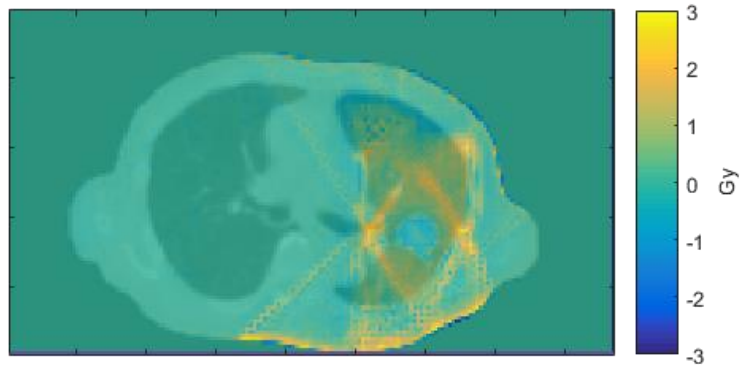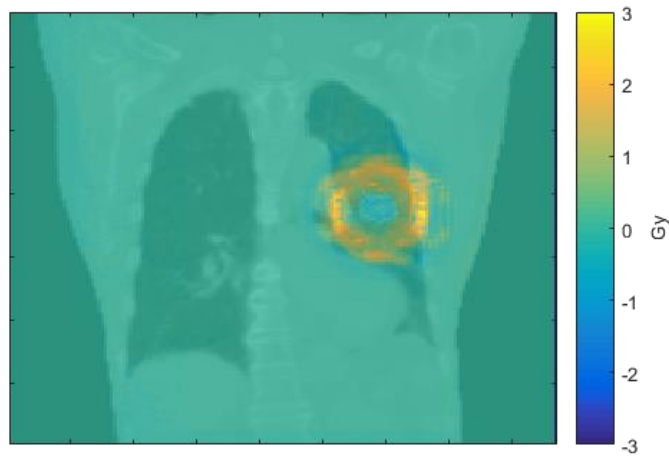(a) 3×3 cm² (b) 5×5 cm² (c) 10×10 cm²

Fig. 5 Calculated clinical dose distributions passing through the isocenter.

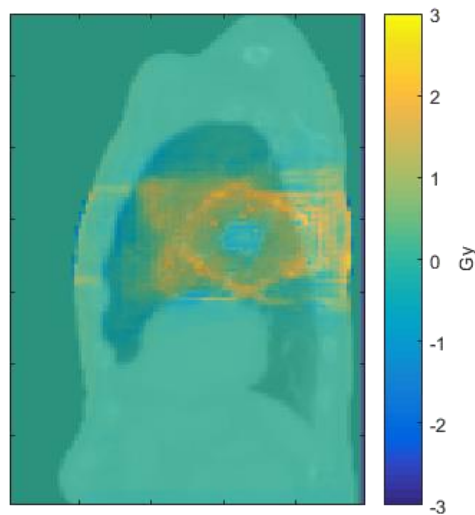Left side: MC, Right side: Acuros XB

(a) axial slice (b) coronal slice (c) sagittal slice

(a)

(b)

(c)

Fig. 6 Subtractions of the dose distribution (Acuros XB − MC).

(a) axial slice (b) coronal slice (c) sagittal slice

Estimation of bovine internal exposure dose from radiocesium contamination

in the Fukushima restricted area by using EGS5

A.   Motegi[1], E. Kobayashi[1], H. Imai[1], C. Shimaoka[1], K. Mutoh[1], T. Kakizaki[1], S. Wada[1], H. Hirayama[2], N. Ito[1], M. Natsuhori[1]

[1]Kitasato University, School of Veterinary Medicine, Aomori 034-0021, Japan
[2]High Energy Accelerator Research Organization, KEK, Ibaraki 305-0801, Japan

Abstract

The purpose of this study is to evaluate internal exposure dose of cattle that lived in Fukushima restricted area. The estimation of the bovine effective dose was based on an originally created mathematical phantom of cattle, the level of the bovine tissue radioactivity (Bq) and absorbed dose rate (Gy/h/Bq) calculated by using EGS5. The internal annual exposure effective dose by ^{40}K was estimated to be 0.23 mSv / year based on the results of absorbed dose rate simulated by EGS5, and the effective dose by the time of oral feeding conditions of ^{137}Cs contaminated feeding (5 kBq / day $\times$ 20 days and then cleaning feed for 50 days) was 14.3 μSv / 70 days.

1. Introduction

The disaster of Fukushima Dai-ichi nuclear power plant of TEPCO after the great east Japan earthquake had strong impact of radiation on the environment in Fukushima and its suburbs. Since the environmental contamination induces other contaminations via food chain, the level of accumulation of radionuclides in livestock may have a potential of the problem of radiation exposure to the animal itself, not only for the food safety in human. However, since there is no research report in the internal exposure of cattle in spite of the level of contamination, we tried to estimate the interaction of the contamination levels on the absorbed dose rate for each of organs and/or tissues in cattle. The target nuclides were ^{137}Cs, ^{134}Cs, and ^{40}K and its estimation was calculated by using EGS5. In addition, for the ^{137}Cs and ^{40}K, we calculate the total absorbed dose of cattle (which corresponds to the effective dose of the people) for a certain period of time and carried out the internal exposure assessment.

2. Materials and methods

A mathematical phantom of cattle (474 kg) was made by using CGview, and the sizes and anatomical positions of organ were obtained by the actual anatomical data and anatomical manual. Elemental composition and density of organs were employed from the human data [1]. The absorbed dose rate   (Gy/h/Bq) was calculated based on the β- and γ-rays of ^{137}Cs, ^{134}Cs, ^{40}K. For ^{40}K, the dose equivalent of the cattle to the annual effective dose of people was estimated by using EGS5, the measured value, and the radiation weighting factor and tissue weighting factor of the people. The levels of radioactivity in organ and/or tissue radioactivity (Bq / kg) of ^{137}Cs, ^{134}Cs, ^{40}K in cattle were measured after daily feeding of radioactive contaminated diet (hay) in Fukushima restricted area within a perimeter of 20 km from the Fukushima Dai-ichi nuclear power plant. These actually measured data was applied for EGS5 calculations. For ^{137}Cs, the effective dose of cattle that was based on the duration of the contaminated feeding by ^{137}Cs was calculated for a predetermined period. Thus the effective dose of ^{137}Cs was based on the record of ^{137}Cs concentration in each organ of totally 70 days

feeding that includes initially 20 days ^{137}Cs contaminated feeding (about 5 kBq / day) and secondary 50 days contamination-free feeding.

3. Results and Discussion

The γ-ray absorbed dose rate was in descending order of ^{134}Cs > ^{137}Cs > ^{40}K about all the specified detection area, whereas the β-ray, the absorbed dose rate was in descending order of ^{40}K > ^{137}Cs > ^{134}Cs. These data were in accordance to the order of the average energy of three nuclides [2]. The cattle phantom contains about 23.8 kBq of ^{40}K in the body, and its annual effective dose was 0.23 mSv. Annual effective dose of a human that has about 3.6 kBq/body of ^{40}K was 0.18 mSv [3]. These results imply that the mean annual effective dose of the people is close to the cattle's in spite that the cattle has about 8 fold heavier. The effective dose of ^{137}Cs for 70 days was 14.3 μSv in the case of continued ^{137}Cs contaminated feeding for 20 days. On the other hand, the effective dose of ^{40}K was 44.1 μSv for 70 days, and the exposure dose of the Chest X-ray of in human is about 0.1mSv for 1 time. Comparing with these data, the effective dose due to this time's condition is thought to be not so high. Moreover, the equivalent dose of muscle (17.9 ~ 21.4 μSv for 70 days) was higher than other organs (4.0 ~ 18.0 μSv for 70 days) since the concentration of measured value of the radiation dose of muscle (823 ~ 8621 Bq in 20 days after starting feeding contaminated food) was higher than other organs (4.1 ~ 425 Bq in 20 days after starting feeding contaminated food). Thus the effective dose was supposed to be predominantly contributed by a large amount of muscle which is the major source of radiocesium (51.9 %).

4. Conclusions

In this study, the effective dose of ^{137}Cs in the case of oral feeding the ^{137}Cs for certain period, and annual effective dose by ^{40}K were estimated in cattle. As a result, we got annual effective dose by ^{40}K in cattle was quite similar to the people. Internal exposure of cattle is not as large as 14.3 μSv in the case of feeding ^{137}Cs contaminated feed in this condition. Based on this example, we can evaluate the effective dose by using actually measured value that may vary by the degree of each contaminated feeding condition.

References

1) ICRP publ 23. Report on the Task Group on Reference Man (1975)
2) J. Peterson, M. MacDonell, L. Haroun, and F. Monette. "Radiological and Chemical Fact Sheets to Support Health Risk Analyses for Contaminated Areas" (2007).
3) H. Sugiyama, H. Terada, K. Isomura, I. Iijima, J. Kobayashi, K. Kitamura, "Internal exposure to ^{210}Po and ^{40}K from ingestion of cooked daily foodstuffs for adults in Japanese cities," Toxicol. **34**. 417-425 (2009).